Vision Res. Vol. 24, No. 6, pp. 533–542, 1984
Printed in Great Britain. All rights reserved
0042-6989/84 $3.00 + 0.00
Copyright © 1984 Pergamon Press Ltd

BINOCULAR DISPARITY MODULATION SENSITIVITY TO DISPARITIES OFFSET FROM THE PLANE OF FIXATION

ROBERT A. SCHUMER* and BELA JULESZ†
A. T. & T. Bell Laboratories, 600 Mountain Avenue, Murray Hill, NJ 07974, U.S.A.

(*Received* 18 *July* 1983; *in final revised form* 14 *October* 1983)

Abstract—Corrugated disparity gratings mounted on depth pedestals were portrayed with random-dot stereograms in order to measure the cyclopean disparity modulation transfer function at various offsets from fixation. We found changes in both sensitivity as well as shape as the magnitude of the pedestal varied. Threshold disparity modulation amplitude curves, plotted as a function of corrugation frequency, became narrower and shifted toward lower frequencies as pedestal size increased. There were stable asymmetries between sensitivities to crossed and uncrossed pedestals; these could be accounted for by assuming each observer to have a constant fixation disparity on the order of 5′ of arc.

Visual psychophysics   Stereopsis

INTRODUCTION

This paper describes an investigation of the detectability of binocular disparity when the spatial distribution of the disparity information changes. Particularly, we studied disparity stimuli placed on disparity pedestals of varying sizes. This study differs from previous investigations of these topics (e.g. Westheimer and McKee, 1978; Westheimer, 1979; Butler and Westheimer, 1978) in that we have employed the random-dot stereogram technique of Julesz (1960) to create our displays, and in that we have used disparity pedestals extending in magnitude to 50′ arc, a range rather larger than has been considered in previously conducted studies.

Sinusoidally modulated disparity gratings, which appear as corrugated surfaces in depth when viewed stereoscopically, have recently been employed to study the spatial pooling of binocular disparity information (Tyler, 1974; Schumer and Ganz, 1979; Tyler and Julesz, 1978). Disparity gratings are created with random dot stereograms (RDS) which portray a sinusoidally modulated surface in depth when viewed stereoscopically, but appear as visual noise to either eye alone. These stimuli are thus "cyclopean" (Julesz, 1971) in that the gratings are purely binocular stimuli. Schumer and Ganz (1979) measured the minimum disparity modulation amplitude (DMA) required to detect a briefly presented disparity grating for a variety of "corrugation frequencies" of disparity modulation. They found a low-frequency fall-off in the DMA sensitivity function, an observation also reported by Tyler and Julesz (1978) and by Rogers and Graham (1982). Tyler (1973; 1975a) also reported the same result with (noncyclopean) line stimuli containing sinusoidal disparity variations. Schumer and Ganz interpreted this as evidence for spatial inhibition between spatially adjacent mechanisms responding to similar disparities.

Schumer and Ganz also reported bandpass DMA threshold elevation following adaptation to a single corrugation frequency disparity grating. These elevation curves might reflect the corrugation frequency sensitivity profiles of component mechanisms subserving perception of depth surfaces. The hypothesis of center-surround antagonism in such a mechanism's spatial disparity weighting function would explain the bandpass rather than lowpass character of the elevation curves. Similar conclusions concerning spatial antagonism were reached by Tyler and Julesz (1978), in a corrugation frequency masking study, and by Anstis *et al.* (1978), who reported a Craik–O'Brien–Cornsweet illusion in depth.

Previously, measurements of the DMA sensitivity curve have been made for disparity gratings having a mean disparity of zero; that is, measurements have always been made at the horopter. The power of the approach through the measurement of DMA sensitivity curves can be more fully exploited if measurements are also made at nonzero mean disparities. These measurements would show how the spatial pooling of disparity varies with changes in the base disparity. We were particularly interested to see if the shape of the DMA sensitivity curve remains the same as base disparity is changed to values other than zero.

As mentioned, these measurements also provide a description of stereoacuity as a function of the spacing of disparity information across space, since higher corrugation frequencies, by definition, exhibit disparity variation at *closer* spatial proximity than do

*Present address: Department of Psychology, New York University, 6 Washington Place, NY 10003, U.S.A.
†To whom requests for reprints should be sent.

lower corrugation frequencies. By performing additional measurements of the DMA sensitivity curve using depth pedestals, we gain a measure of how stereoacuity changes when the disparity information is presented away from the fixation plane.

A final reason for performing such measurements was to see whether the very large upper depth limits found with brief presentations of RDS flat stereosurfaces (Tyler and Julesz, 1980), far in excess of Panum's area for fusion of line targets (Ogle, 1950), could still be reached when the task requires spatial *resolution* of large disparity stereo surfaces. Indeed, Richards (1977) has questioned the ability of human observers to perform more than the most coarse discriminations at large disparities with random-dot stereograms. To anticipate: we find that the ability to perform stereoscopic depth discrimination is present at large disparities, but it is necessary that the spatial parameters of the stimulus be optimally chosen. In particular, the corrugation frequency of the stimulus must be low.

METHODS

Dynamic random dot stereograms were presented on a pair of Hewlett-Packard 1300A cathode ray oscilloscopes (P4 phosphor) under control of a PDP-11/20 computer and special display hardware designed by W. Kropfl. The special hardware allowed a 16-fold increase in the rate at which dots were presented. The screens were covered with crossed polarizing material, their images superimposed with a beam-splitting mirror, and they were viewed with crossed polarizing filter glasses so that each eye saw only one screen.

The dot fields were composed of 100 horizontal lines, each consisting of 500 potential dot positions. 6.25% of all positions, for a total of 3125 dots, were at random brightened during each 25 msec frame. The screens were viewed from 50 cm and the dot fields subtended 8 deg horizontally and 10 deg vertically (except as described below); dot density was in consequence approximately 40 dots/deg^2. The spacing of the dot positions was 6′ vertically and 1′ horizontally, although each actual brightened dot had a diameter of 6′; horizontally adjacent dots were thus superimposed to some extent.

Disparity gratings were formed by electronically adding to the voltage that controlled the horizontal position of each row of dots the output of a cyclically repeating digital-to-analog converter whose cycle-time was synchronized to the vertical sweep of the display (cf. Schumer and Ganz, 1979). The 5-V peak amplitude output signal of the D–A converter was attenuated so that the *resolution* of horizontal shifting of rows of dots (that is, of disparity) was quite high, usually on the order of about 0.5% of the threshold shift (threshold disparity) in any given condition. The temporal waveform of the output of the D–A, and therefore the spatial distribution of horizontal shifts had the form of a sine wave, as is shown in Fig. 1. When stereoscopically viewed, this resulted in the percept of a surface that was uniform in depth across any horizontal row, but which was modulated sinusoidally about the vertical axis of the dot fields. Schumer and Ganz (1979) show a photograph of this stimulus on a different display system.

The corrugation frequency and modulation depth of the disparity grating were determined by the spatial frequency and amplitude of the sinusoidal shift. Occasionally, in order to obtain higher corrugation frequencies without excessive sacrifice of vertical spatial fidelity, the spacing between rows of dots was halved, producing a field 5 deg in height. In

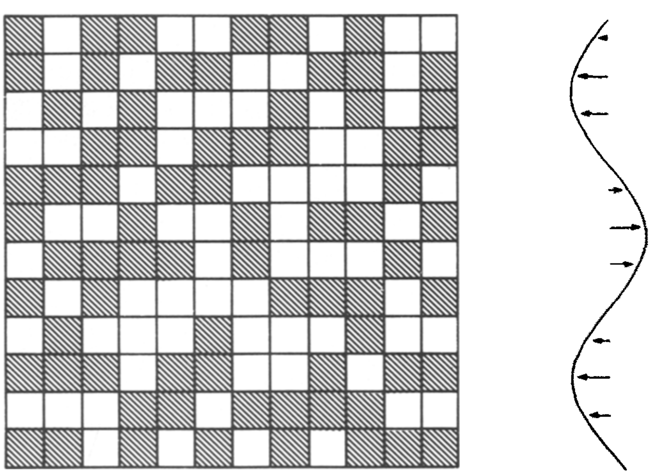

Fig. 1. Schematic for the construction of a stereoscopic disparity grating. Random dots (here shown at an exaggerated scale) are presented to one eye. The other eye views the same dot pattern, but adjusted so that each horizontal row is positioned slightly to one side or the other of adjacent rows. The pattern of shifts across all rows is a sinusoid whose amplitude and frequency can be varied. These parameters are referred to as disparity modulation amplitude (DMA) and corrugation frequency, respectively.

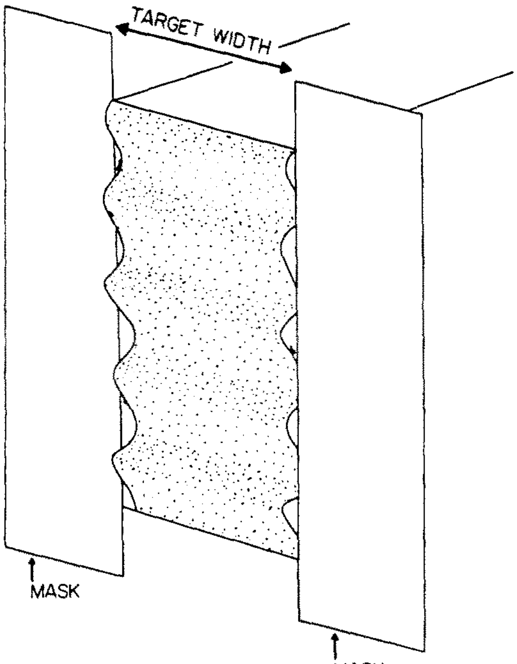

Fig. 2. The stimulus appears as a corrugated surface in depth, with a dotted texture. The lateral edges are masked in the actual display so that monocularly present edge ripples are not seen, and the spacing of possible dot positions is substantially smaller than the width of an actual dot. The stimulus is thus "cyclopean" (Julesz, 1971).

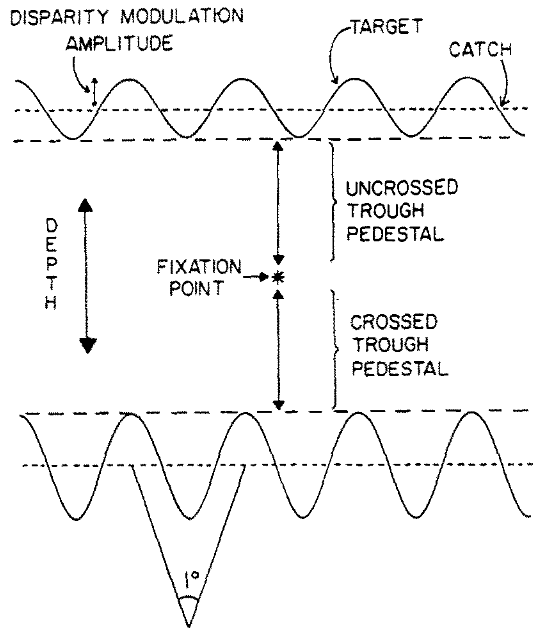

Fig. 3. Features of experimental procedure. Disparity gratings of various corrugation frequencies were presented at a range of offsets in depth from the fixation point, in both the divergent (uncrossed) and convergent (crossed) directions. These offsets are referred to as "trough pedestals" or more simply, just as "pedestals". Disparity gratings were always presented with their *troughs* (points of smallest absolute value of disparity) placed on the pedestal. For different disparity modulation amplitudes, consequently, the pedestal was fixed, but the *mean* disparity across space was varied. A catch stimulus had no corrugation but was a flat surface with the mean disparity of the grating, and thus could vary in magnitude from trial to trial.

this case the percentage of brightened dot positions was also reduced by half, thus maintaining a constant dot density, although changing the degree of overlap of brightened dots.

Masks were placed at the sides of the screens to occlude the lateral edges of the dot fields and thus to eliminate any monocular cue to the presence or direction of sinusoidal modulation. The appearance of the stereoscopic stimulus as viewed by the observer is illustrated in Fig. 2. A number of features of our stimulus arrangement and psychophysical procedure are illustrated in Figs 3 and 4. When presenting disparity gratings with nonzero mean disparities, a uniform horizontal displacement of the entirety of one eye's dot field was added to the sinusoidal displacement, resulting in a depth grating mounted on a uniform depth offset. When such an offset pedestal was used, its magnitude was kept constant within each condition, and the grating disparity was added to this offset. To emphasize this point, Fig. 3 refers to these offsets as *trough* pedestals, and shows disparity gratings added to them. The pedestal values reported in the Results section are these trough pedestal values, which did not vary with the DMA from trial to trial within a condition, and always refer to the smallest disparity presented for that condition, although the test DMA may have varied considerably. In the remaining figures and text, we will usually refer to these offsets simply as pedestals, although we will always mean trough pedestals.

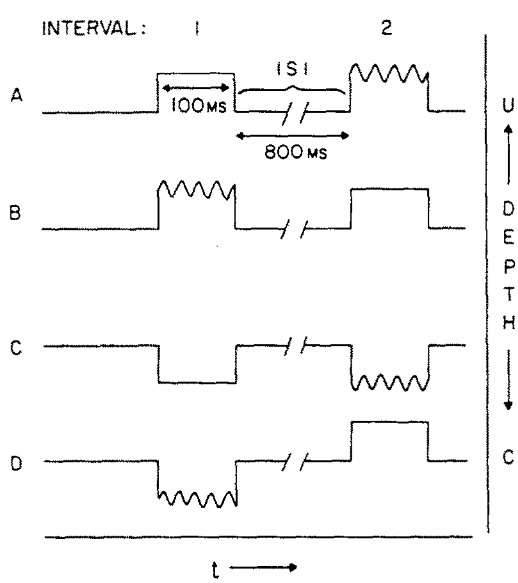

Fig. 4. Schematic of interval structure. Two 100 msec intervals were separated by 800 msec. The fixation point was on whenever the stimulus was off. The grating could be in either interval, and the catch could be either crossed or uncrossed, independent of the disparity sign of the test grating with which it was paired.

The observer initially fixated a small bright dot in an otherwise dark field. When fixation was felt to be stable, the observer initiated a trial consisting of two 100 msec stimulus intervals separated by 800 msec of the dark field together with the fixation point. Both intervals were composed of 4 *different* 25 msec frames of random dots, although each of the 4 stereoscopic frames portrayed the same *stereoscopic* stimulus. The test disparity grating, mounted on pedestals of varying sizes, appeared at random in either the second or the first of the two stimulus intervals, while in the other interval was presented a catch stimulus, which consisted of a flat disparity pedestal but no grating, as indicated in Fig. 4(a) and (b).

The disparity grating was presented in random spatial phase from trial to trial. The task was to identify the interval containing the disparity grating. A computer-controlled forced-choice staircase, chosen to impose a fairly stringent criterion on the observer, modified the DMA according to the rule: 4 correct in a row for a step down, 1 wrong for a step up. This rule causes the staircase to converge on the 84% point of the psychometric function*. Incorrect responses were signalled to the observer by a tone.

Two independent and randomly interwoven concurrent staircases were maintained, one for test gratings on crossed (near in depth) disparity pedestals, the other for test gratings on uncrossed (far in depth) disparity pedestals (see Fig. 3). Finally, on any trial, independently of whether the crossed or uncrossed staircase (target grating) was used, the catch stimulus (pedestal only) was chosen at random to be either crossed [Fig. 4(c)] or uncrossed [Fig. 4(d)]. This technique was employed to encourage the observer to maintain fixation upon the white dot throughout the 1 sec trial in order to have the best opportunity to see stimuli in both intervals. The evidence that this strategy was in fact successful was provided by the observation that if the observer wilfully deviated his or her fixation from the fixation point, there was a marked and subjectively noticable reduction of performance. In retrospect, this is to be expected based on the sharp changes in sensitivity with changes in pedestal size (see Fig. 12).

The catch stimulus was not equal in disparity magnitude to the trough pedestal used for the disparity grating. Rather, it was the trough pedestal *plus* the current staircase value of the mean-to-peak DMA of the test grating with the *same* depth polarity (crossed or uncrossed) as the catch stimulus, regardless of whether that disparity grating was presented on that particular trial. Thus, discrimination of catch from target stimuli could never be based on differences in mean disparity alone, even when DMA was quite large.

Each of the points shown in the following graphs is based on at least 3 and usually 6 repetitions of the staircase, on separate days, each staircase involving roughly 100 trials (at least 11 staircase reversals). There were two observers: one of the authors (R.S.) and a naive assistant. Both were highly practiced in the tasks described above; considerable practice was found to be necessary before performance stabilized. We judge this to have been so largely because of the strain and fatigue accompanying the observer's effort to maintain fixation and make detailed spatial resolution judgements throughout the period of stimulation. The trials were perhaps unusually "potent" in that they consisted of two temporally separated, large, bright sheets of temporally and spatially complex visual noise with compelling and often large binocular disparities. The observer, of course, had to learn to focus on the required task of spatial comparison while ignoring many other, "distracting" aspects of the stimuli. This seems to have required the development of novel attention strategies. Also, there are reports, using conventional line stereograms, of dramatic improvements over time in stereoscopic sensitivity (Fendick and Westheimer, 1983), and it is possible that this effect underlies, in part, our observation.

RESULTS

For observer C.G., DMA thresholds as a function of corrugation frequency are shown in Figs 5–9 for disparity pedestals of 0, 20′, 30′, 40′, and 50′, respectively. The plots are on logarithmic coordinates, with the reciprocal of threshold plotted on the ordinate. Looking first at Fig. 5, the peak sensitivity at the zero pedestal occurs at a corrugation frequency of about 0.3 c/deg. At this corrugation frequency, threshold is about 10″ of arc. As corrugation frequency increases, sensitivity drops off. As corrugation frequency decreases, sensitivity also drops off. For reasons to be given shortly, we feel that this is not a consequence of the small number of cycles that were visible at the lowest frequencies tested.

Figure 6 shows data for pedestals of 20′. Note that the ordinate scale has been altered. Sensitivity has

*The point on the psychometric function (probability-of-seeing curve) that a staircase rule estimates is calculated by solving for the probability at which a step "up" is equally likely to a step "down" in the staircase. Since we require 4 correct responses in a row for a step "down" (decreasing disparity modulation) while a step "up" (increased disparity) is taken following either one incorrect response or one, two, or three correct responses followed by one incorrect response, the equation to be solved is

$$p(i)^4 = [1 - p(i)] + p(i)[1 - p(i)] + p(i)^2[1 - p(i)] + p(i)^3[1 - p(i)]$$

where $p(i)$ is the probability of a correct response at disparity modulation amplitude i. This can be rewritten as

$$p(i)^4 = [1 - p(i)] \times [1 + p(i) + p(i)^2 + p(i)^3].$$

This is readily solved using numerical approximation to yield $p(i) = 0.84$.

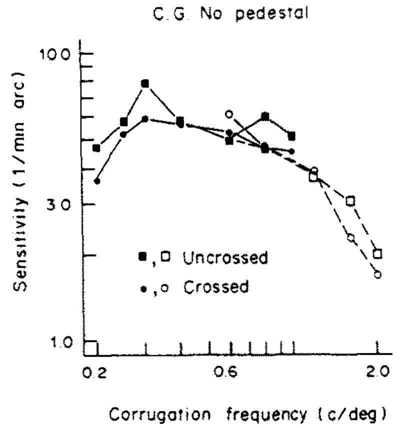

Fig. 5. Results of threshold measurements for observer C.G. with no pedestal. Square symbols: uncrossed disparity; circular symbols: crossed disparity. Open symbols (and dashed lines) show data taken with display having one-half the vertical extent as for filled symbols (with solid line), as explained in text. Peak sensitivity of 8 corresponds to 7.5″ of arc of disparity modulation amplitude.

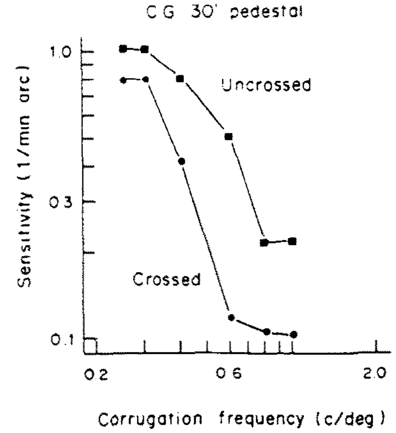

Fig. 7. As for Fig. 5, but with pedestal of 30′ arc of crossed or uncrossed disparity. Circles are for crossed, squares are for uncrossed disparity pedestals.

fallen off uniformly, and the sensitivity to crossed and to uncrossed disparities has become unequal. Notice also that the high frequency loss has become much more severe: in going from 0′ to 20′ pedestals, the ratio of sensitivity at the peak frequency to that at a corrugation frequency 2 octaves higher has grown from about 3:1 to about 20:1. At 30′ pedestals, as shown in Fig. 7, high frequency loss is even more severe, and this trend continues as pedestal size is further increased (Figs 8 and 9).

Figure 10 shows all of the data from Figs 5 to 9 in one plot, with one ordinate scale, for ease of comparison. It can be appreciated from this plot, (1) that overall sensitivity to disparity modulation becomes lower, at all frequencies, as pedestal size increases. (2) For this observer, sensitivity to high corrugation frequency worsens at a faster rate than to moderate corrugation frequency. This is indicated by the steeper slope of the high frequency portion of the

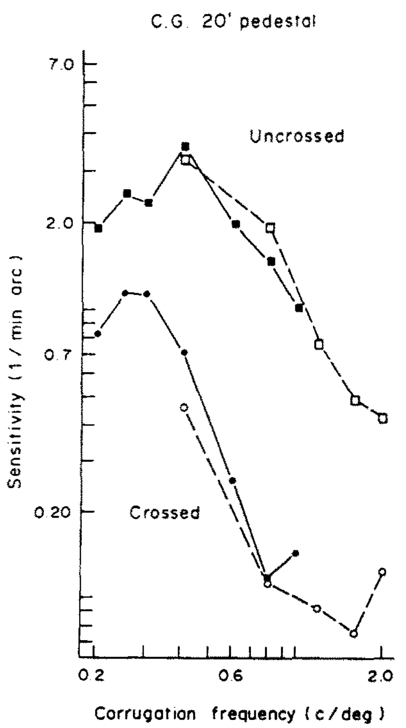

Fig. 6. As for Fig. 5, but with pedestal of 20′ arc of crossed or uncrossed disparity.

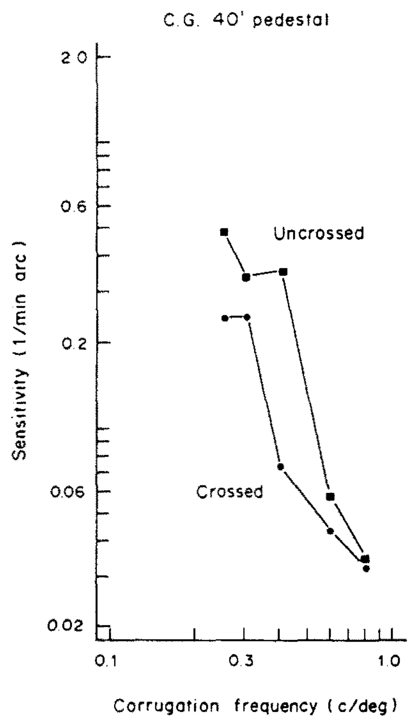

Fig. 8. As for Fig. 5, but with pedestal of 40′ arc of crossed or uncrossed disparity. Circles are for crossed, squares are for uncrossed disparity pedestals.

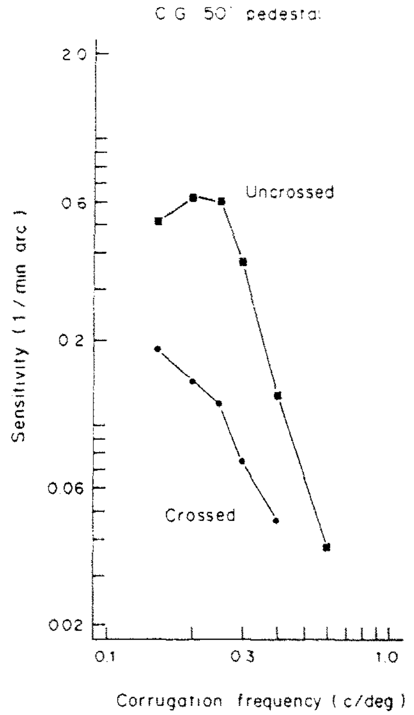

Fig. 9. As for Fig. 5, but with pedestal of 50′ arc of crossed or uncrossed disparity. Circles are for crossed, squares are for uncrossed disparity pedestals.

curves as they proceed from top to bottom. (3) The low frequency portion of the curves flatten out as pedestal size increases. That is, the relative low frequency attenuation in sensitivity progressively disappears. This is one reason why the low frequency loss at the zero pedestal was not an artifact of the small number of cycles, since, had it been, we would expect it to occur at all pedestals. Also, Tyler and Julesz (1978) observed low frequency sensitivity loss for disparity gratings modulated about the horopter using a stimulus field subtending 50 deg of visual angle, and in that case there certainly was not a problem due to small cycle-number. In addition, we have previously found (Schumer and Julesz,*) that sensitivity to disparity gratings at the horopter is not affected by reductions in the number of cycles until there are less than about 3 cycles presented. Tyler (1975a) reported the same result with nonrandom-dot corrugated figures. (4) The asymmetry in sensitivity to crossed and uncrossed disparity pedestals persists at all pedestal sizes of 20′ or larger. C.G. was uniformly more sensitive to uncrossed than to crossed pedestals. We return to this observation later on. (5) Finally, there is some indication that the peak sensitivity may shift to lower corrugation frequencies as pedestal size increases, but our apparatus could not be used to test this in the very low frequency range.

Figure 11 shows data for observer R.S. at the zero pedestal and at 25′ and 40′. Many of the same tendencies in the data are evident for this observer, although R.S. shows uniformly greater sensitivity to crossed than to uncrossed pedestals. Two differences in the data are noteworthy. First, the tendency for peak sensitivity to shift to lower corrugation frequencies as pedestal increases is again in evidence, although for R.S. the pattern is rather more compelling than for C.G. Second, as pedestal increases, the slopes of the high frequency portion of the curves do not appear to change as dramatically as they did for C.G. Notice that a vertical shift of the curves plus a horizontal shift (to compensate for the change in peak sensitivity) brings the curves into rather good alignment.

DISCUSSION

Fixation disparity and asymmetric disparities

C.G. was uniformly more sensitive to disparity modulation when mounted on uncrossed than on crossed pedestals, while the opposite was true for R.S. In fact, each observer who has performed this task shows a small but reliable preference, in the form of lower thresholds, for one or the other pedestal

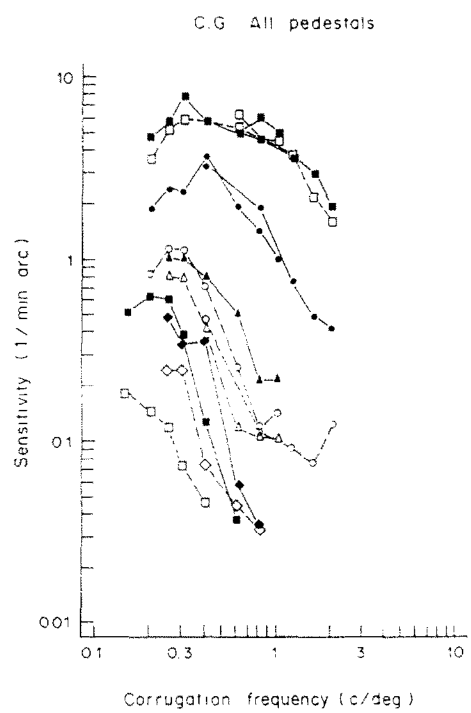

Fig. 10. Summary of data for C.G., plotted on one graph for comparison across pedestals. Squares: no pedestal. Circles: 20′ arc pedestal. Triangles: 30′ arc pedestal. Diamonds: 40′ arc pedestal. Squares: 50′ arc pedestal. Solid symbols and solid lines: uncrossed pedestals. Open symbols and dashed lines: crossed pedestals. Note greater sensitivity to uncrossed pedestals than to crossed pedestals.

*Schumer R. A. and Julesz B. (1980) Limited area integration of binocular disparity detectors in global stereopsis. Paper presented at: *Topical Meeting on Recent Advances in Vision, Opt. Soc. Am.*, Sarasota, FL.

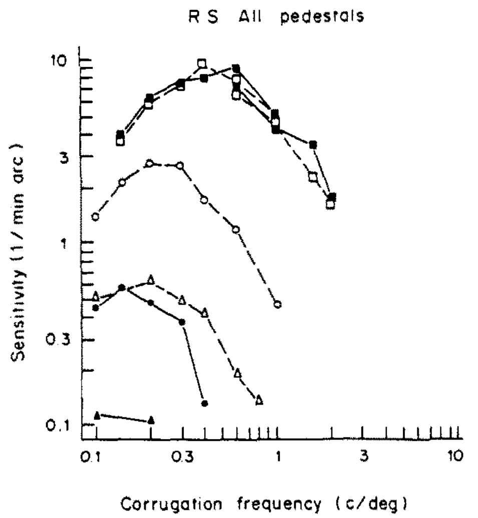

Fig. 11. Data for three pedestals for R.S. Squares: no pedestal. Circles: 25′ arc pedestal. Triangles: 40′ arc pedestal. Solid symbols and solid lines: uncrossed pedestals. Open symbols and dashed lines: crossed pedestals. Note greater sensitivity to crossed pedestals than to uncrossed pedestals, opposite to pattern seen in Fig. 10.

type. We have observed that the asymmetry in sensitivity may in part be accounted for by assuming each observer to have an idiosyncratic fixation disparity on the order of several minutes of crossed or uncrossed disparity. Such a deviation from perfect convergence would have the consequence of causing the nominal pedestals used here to be systematically shifted in depth in a constant direction for each observer.

For C.G., we estimated fixation disparity by the following procedure: we replotted the data of Fig. 10 so that pedestal size was on the x-axis; different curves were plotted for each different corrugation frequency. Then we shifted each plot, sliding the (lower threshold) uncrossed pedestal data toward smaller pedestals, and the crossed pedestal data by an equal amount toward larger pedestals. We found that it was possible, except at the largest pedestals used, to cause the two curves, for crossed and uncrossed pedestals, to overlap to a considerable degree. The shifts required to do this were always between 4 and 7 min arc in the crossed direction (meaning fixation error in the uncrossed direction).

Figure 12 shows the original crossed and uncrossed data for C.G., for two corrugation frequencies, 0.4 c/deg and 0.8 c/deg, replotted as described above, (open symbols, dotted lines), and also the same data "corrected" assuming a 6 min arc uncrossed fixation disparity (solid symbols, solid lines).

The correction results in much closer agreement between the sensitivites to crossed and uncrossed pedestals. A correction for R.S. of 4 min of crossed disparity gave similarly satisfactory alignment of the two sets of curves. The asymmetries between crossed and uncrossed disparities may thus reflect no more than a systematic misconvergence.

It is possible that this misconvergence is peculiar, in either magnitude or even its existence, to the conditions of our experimental situation. We should however point out that the asymmetries observed were reliable for each observer in sign and magnitude across corrugation frequencies and across many months of data collection, although they differed in both sign and magnitude across observers. It might further be mentioned that one of the authors (B.J.), for whom some data was collected on the present task, has shown the same asymmetry of preference,

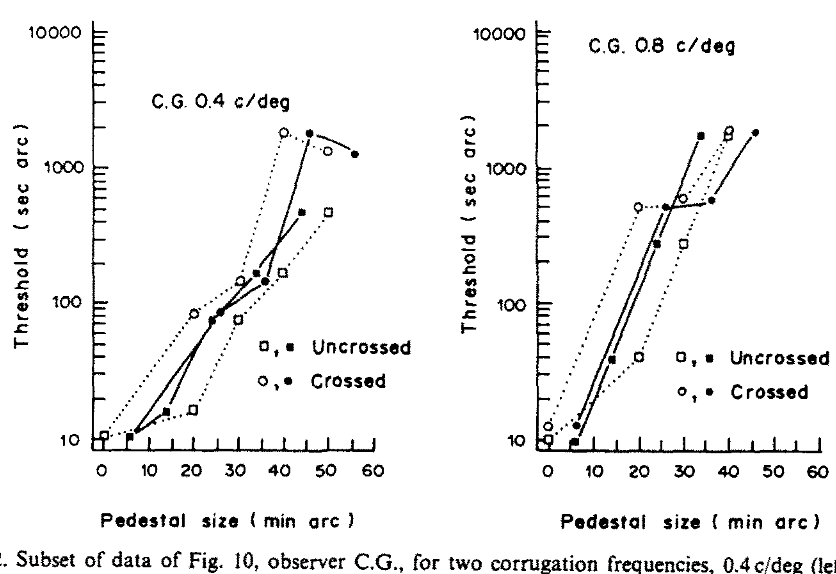

Fig. 12. Subset of data of Fig. 10, observer C.G., for two corrugation frequencies, 0.4 c/deg (left) and 0.8 c/deg (right), "corrected" assuming a fixation disparity of 6′ arc uncrossed vergence angle. Dashed lines for crossed (circles) and uncrossed (squares) pedestals; solid lines are corrected data. Nature and rationale of correction is described in text.

favoring uncrossed disparity, in previous studies, spanning several years of time (e.g. Julesz and Chang, 1976).

Fixation disparities have been previously reported and discussed by Ogle (1950; pp. 69–93). For observer K.N.O. he reported a crossed fixation disparity of about 3.7′ arc (at 40 cm), a value in the same range as our estimates for C.G. and R.S., although Ogle's measurements were made using a rather different technique than ours.

The cyclopean transfer characteristic

Because our data have been plotted in logarithmic coordinates, a gain change in an otherwise constant disparity "transfer characteristic" across different pedestals would appear as a simple vertical displacement of the same frequency response curve. There is, in fact, a systematic displacement of the vertical position of successive curves as we proceed from smaller to larger pedestals. This general decline in DMA sensitivity as pedestal size increases indicates that resolution of disparity information for each spatial arrangement depends upon the disparity offset of that information.

However, superimposed upon this sensitivity reduction with increasing pedestal size is an authentic change in shape of the curves. For C.G., this change in shape is most pronounced at higher frequencies, while for R.S. the change is somewhat greater at lower frequencies. It is of course possible for a single mechanism to change transfer characteristic with changes in the dynamic level of stimulation. An alternative and perhaps simpler view would be to suppose that at different pedestals, different detection mechanisms become most sensitive and, in threshold measurements, reveal their own spatio-disparity pooling properties. In other words, it is possible that sensitivity at different depth offsets from the fixation plane is subserved by differently organized mechanisms. At present we lack evidence which would discriminate these two alternatives. The simplest approach would be to attempt selective adaptation of individual mechanisms at different offsets from fixation, but difficulty in controlling eye movements makes this impractical.

Several particular interpretations may be offered in view of the kinds of distortions seen in the family of curves in Figs 10 and 11. *First*, the decreased sensitivity with increasing pedestal size may reflect a broadening, in the disparity domain, of the size of disparity detectors with increases away from zero disparity. Another possibility is that the range of disparities over which pooling takes place is an increasing function of the mean value of presented disparities. In either case, the finding is in line with previous reports that the discriminability in depth of line targets declines as targets are moved in depth away from fixation. In particular, Blakemore (1970) reported that depth discrimination depends exponentially upon depth offset from the horopter (that is, with pedestal size, in the present terminology). In Fig. 12, the same relationship can be seen. The exponent is different for the two corrugation frequencies of Fig. 12, and varied with corrugation frequency in general. Specifically, if D is depth discrimination in degrees, P is pedestal size in degrees, x is a constant dependent on corrugation frequency, and t is the $\log_x$ of threshold at zero pedestal (at the horopter), then the data of Fig. 12, as well as Blakemore's (1970) data [Fig. 5(b) and 7] are described by a function of the form

$$D = x^{(P+t)}.$$

In the absence of a thorough model of the detection of disparities at offsets from the fixation point, we see no point in speculating on the significance of this relation; it nevertheless has now been shown to hold using two quite different methodologies, and deserves further study.

Second, in light of the tendency toward improved relative sensitivity in the low frequency portions of the curves as pedestal increases, there appears to be a diminished amount of spatially lateral antagonism between disparity detectors (Schumer and Ganz, 1979) for low frequency mechanisms at large pedestals as compared to mechanisms for the same frequencies but at smaller pedestals. This would account for the observed change in shape. It could also be that with large pedestals sensitivity to low frequencies is improved relative to middle frequencies because of a spatial broadening of the largest spatial disparity weighting function at larger pedestals.

Relation to earlier data on large depth limits

As mentioned in the introduction, Richards (1977) has presented evidence that depth perception with random dot stereograms is impovershed compared to stereopsis with classical line stimuli. This conclusion, however, is probably mitigated by the particular stimulus configuration in that study: bars in depth 20′ arc wide. If we consider a single bar in depth to be comparable to a single half-cycle of a disparity grating, this corresponds to a corrugation frequency of about 1.5 c/deg. Richards found that observers viewing 200 msec RDS presentations of this stimulus with disparities greater than 10′–15′ arc had considerable difficulty seeing the bar in depth. In contrast, when stimuli of identical size but composed of simple bars of light were used, observers could differentially perceive the depth of different disparities up to about a degree of arc. Richards concluded that monocular cues are an essential part of stereoscopic processing, and that random dot stereograms, which by design lack monocular cues, are an unnatural stimulus yielding only rough and inadequate stereoscopic sensations.

Based on data reported in this paper, we suggest that Richards' result was due to his use of very narrow bars, which correspond to a *high* corrugation frequency. From Figs 10 and 11 we see that stereoscopic resolution is severely impaired at corrugation frequencies of 1.5 c/deg. Nevertheless, considerably more sensitive performance is possible *if the corrugation frequency of disparity modulation is chosen properly*. Indeed, observer C.G. could discriminate a flat surface with 52′ arc disparity from a surface modulating between 50.3′ arc and 53.7′ arc of disparity, but *only* if the spatial separation between peaks and troughs of the modulated surface was 2.5 deg (Fig. 8).

We suspect that had Richards used broader bars, he would have found improved performance at larger disparities. Certainly, spatial resolution of disparity gratings at its best is poorer, by about a factor of 10, than resolution of luminance gratings, but this need not reflect a limitation of random dot stimulation. Rather, it can be regarded as a methodological advantage of such stimulation in that it reveals the spatial organization of disparity processing uncontaminated by luminance domain mechanisms.

Relation to earlier stereoacuity data

Westheimer (1979) and Westheimer and McKee (1978) have reported stereoacuity measurements for thin line stimuli mounted upon small depth pedestals. Westheimer (1979) used a stimulus which consisted of 3 vertical lines spaced 10′ arc apart. The flanking lines remained in the plane of fixation, and the central line was presented for 500 msec at a pedestal disparity of either 0, 1′ or 2′ arc crossed or uncrossed disparity. After 200 msec of a dark interval, the 3 lines were presented again but with the central line displaced in depth by a small amount. Threshold for detecting the direction of this shift was found to increase steeply as the pedestal changed from only 0 to 1′ arc. If, however, the flanking lines *shared* the pedestal value of the test lines, there was no increase in threshold for nonzero pedestals.

Westheimer concluded that the elevation in the first case was not due to poorer ability to discriminate disparities seen in depth, but rather was due to poorer ability to make depth difference judgements between the middle and outer lines of the target configuration when they had even a small relative disparity.

We can compare our findings with Westheimer's. We have shown, *first*, that the decline in stereoacuity holds for pedestals on the order of tens of minutes of arc, supplementing Westheimer's finding of an effect on the order of minutes of arc. *Second*, we have found that the lateral distribution of disparity information across space is indeed an important factor in determining stereoacuity, as Westheimer concluded. We add to this the finding that varying the spatial separation of disparity information results in a U-shaped function, with relative interference occurring at both near displacements as well as at far displacements. We cannot say whether the low frequency decline in sensitivity results from active inhibition or from the absence of a reference disparity at sufficiently close separations. *Third*, we have shown that the nature of the effect of lateral displacement of nearby disparities is dependent on the pedestal used.

In light of these remarks we suggest that Westheimer's results may usefully be viewed as a sample of the overall stereoacuity surface, derived from the high corrugation frequency portion of that surface. Ten minute of arc displacements between flanking and test lines approximates a 3 c/deg surface. At this "equivalent" corrugation frequency we would expect deleterious effects of even small pedestals. Indeed, this interpretation is consistent with data of Butler and Westheimer (1978), who found that the inhibitory effect of the flanking lines was greatest when the lateral displacement of flanking lines was 2′ arc, but declined for larger separations (lower equivalent corrugation frequencies). Data were only reported in that study for the no pedestal case.

In the Westheimer (1979) study, when the flanking lines were at the pedestal of the test line, it may have been that the effective corrugation frequency was determined by the spatial relationship of the test line to surrounding markers lying in the plane of fixation, laterally separated by about 15′ arc, although not visible when the stimulus was presented. These external markers could have provided the reference for disparity comparisons across space.

The analysis of form-in-depth

In Marr's (1982) framework for the representation of visual objects, different visual processes, such as stereopsis or movement sensitive mechanisms, deliver separate but converging inputs to higher centers. The collection of such inputs is incorporated into a general representation of shape.

The existence of stereopsis from random dot patterns (Julesz, 1960) demonstrates that stereopsis can provide information about shape which is independent of the shape information given by monocularly identifiable features. It follows that there must occur the extraction of shape information by purely stereoscopic means. Problems similar to those encountered in the analysis of form from luminance variations, such as size resolution and edge localization, must also be solved for the stereoscopic case. We therefore suggest that a possible role for the mechanisms proposed here and by Schumer and Ganz (1979) is as "hypercyclopean channels" (Tyler, 1975b; Julesz and Schumer, 1981) whose function would be to aid in the early extraction of blob and contour information from purely stereoscopic depth information.

Acknowledgements—We thank W. Kropfl for programming and equipment assistance. R.A.S. was supported in part by a postdoctoral fellowship from NIH (EY 5511) during the preparation of this manuscript.

REFERENCES

Anstis S. M., Howard I. P. and Rogers B. (1978) A Craik–O'Brien–Cornsweet illusion for visual depth. *Vision Res.* **18**, 213–217.

Blakemore C. (1970) The range and scope of binocular depth discrimination in man. *J. Physiol.* **211**, 599–622.

Butler T. W. and Westheimer G. (1978) Interference with stereoscopic acuity: spatial, temporal, and disparity tuning. *Vision Res.* **18**, 1387–1392.

Fendick M. and Westheimer G. (1983) Effects of practice and the separation of test targets on foveal and peripheral stereoacuity. *Vision Res.* **23**, 145–150.

Julesz B. (1960) Binocular depth perception of computer-generated patterns. *Bell System Tech. J.* **39**, 1125–1162.

Julesz B. (1971) *Foundations of Cyclopean Perception.* Univ. of Chicago Press, Chicago.

Julesz B. and Chang J.-J. (1976) Interaction between pools of binocular disparity detectors tuned to different disparities. *Biol. Cybernet.* **22**, 107–119.

Julesz B. and Schumer R. A. (1981) Early visual perception. *Ann. Rev. Psychol.* **31**, 575–627.

Marr D. (1982) *Vision.* Freeman, San Francisco, CA.

Ogle K. N. (1950) *Researches in Binocular Vision.* Saunders, Philadelphia, PA.

Richards W. (1977) Stereopsis with and without monocular cues. *Vision Res.* **17**, 967–970.

Rogers B. and Graham M. (1982) Similarities between motion parallax and stereopsis in human depth perception. *Vision Res.* **22**, 261–270.

Schumer R. A. and Ganz L. (1979) Independent stereoscopic channels for different extents of spatial pooling. *Vision Res.* **19**, 1303–1314.

Tyler C. W. (1973) Stereoscopic vision: cortical limitations and a disparity scaling effect. *Science* **181**, 276–278.

Tyler C. W. (1974) Depth perception in disparity gratings. *Nature* **251**, 140–142.

Tyler C. W. (1975a) Spatial organization of binocular disparity sensitivity. *Vision Res.* **15**, 583–590.

Tyler C. W. (1975b) Stereoscopic tilt and size aftereffects. *Perception* **4**, 187–192.

Tyler C. W. and Julesz B. (1978) Spatial frequency tuning for disparity detectors in the cyclopean retina. *J. opt. Soc. Am.* **68**, 1365.

Tyler C. W. and Julesz B. (1980) On the depth of the cyclopean retina. *Expl Brain Res.* **40**, 196–202.

Westheimer G. (1979) Cooperative neural processes involved in stereoscopic acuity. *Expl Brain Res.* **36**, 585–597.

Westheimer G. and McKee S. P. (1978) Stereoscopic acuity for moving retinal images. *J. opt. Soc. Am.* **68**, 450–455.